Second Universal Limit of Wave Segment Propagation in Excitable Media

A. Kothe, V. S. Zykov, and H. Engel
Institut für Theoretische Physik, Technische Universität Berlin, D-10623 Berlin, Germany
(Received 12 June 2009; published 9 October 2009)

A free-boundary approach is applied to derive universal relationships between the excitability and the velocity and the shape of stabilized wave segments in a broad class of excitable media. In the earlier discovered low excitability limit wave segments approach critical fingers. We demonstrate the existence of a second universal limit (a motionless circular shaped spot) in highly excitable media. Analytically obtained asymptotic relationships and interpolation formula connecting both excitability limits are in good quantitative agreement with results from numerical simulations.

DOI: 10.1103/PhysRevLett.103.154102 PACS numbers: 05.45.−a, 05.65.+b, 47.54.−r, 82.40.Bj

Wave processes in excitable media play an important role in a variety of different physical, chemical, and biological systems like cardiac tissue, catalytic surface reactions, semiconductor and gas discharge devices, or concentration waves in the Belousov-Zhabotinsky (BZ) reaction [1–5]. Many basic features of waves propagating in excitable media can be analyzed by means of a generic two-component reaction-diffusion model of the form [5]

$$\frac{\partial u}{\partial t} = D\nabla^2 u + F(u,v), \quad \frac{\partial v}{\partial t} = D_v \nabla^2 v + \epsilon G(u,v), \quad (1)$$

where the variables u and v represent the propagator and controller species, respectively. Typically the nullcline $F(u, v) = 0$ is a nonmonotonic function creating the possibility for undamped wave propagation. The second nullcline $G(u, v) = 0$ is monotonic and intersects the first one at only one point (u_0, v_0) as illustrated in Fig. 1. Below the functions $F(u, v)$ and $G(u, v)$ are taken in the form used previously [6–8]:

$$F(u,v) = 3u - u^3 - v, \qquad G(u,v) = u - \delta, \quad (2)$$

where the constant δ determines the uniform rest state as $(u_0, v_0) = (\delta, 3\delta - \delta^3)$, which is stable if $\delta < -1$.

If the propagator diffusion coefficient $D < D_v$ and the functions $F(u.v)$ and $G(u, v)$ satisfy certain conditions, a spatially homogeneous solution $u(x, y, t) = u_0$ and $v(x, y, t) = v_0$ in a two-dimensional medium can be unstable and develops into Turing patterns [9] or localized particle like spots [10,11]. However, in models for neuromuscular tissues, catalytic surface reactions or BZ reaction with fixed catalyst the controller species does not diffuse, i.e., $D_v = 0$. In this important case considered below localized traveling wave segments also have been observed, but only under a stabilizing feedback [12,13], which, however, can be noninvasive [14].

To explain the appearance of such a solution, note that the system (1) and (2) transforms into a bistable medium if $\epsilon = 0$, since then (u_e, v_0) represents another stable steady state. Here u_e is the largest root of the equation $F(u, v_0) = 0$. The bistable system is able to support stationary propagation of a front, which corresponds to a transition from one steady state to another [2,15]. The velocity of a planar front depends on the controller value v_0 and vanishes at $v_0 = v^*$. The front propagation is supported if the deviation $\Delta \equiv v^* - v_0 < \Delta_c$. If $\Delta \ll \Delta_c$ the front velocity c_p is proportional to Δ and is given by

$$c_p(v_0) = \alpha\sqrt{D}\Delta. \quad (3)$$

The constants α, v^*, and Δ_c are determined by $F(u, v)$ and for $F(u, v)$ defined in Eq. (2), $\alpha = 1/\sqrt{2}$, $v^* = 0$, and $\Delta_c = 2$.

If $0 < \epsilon \ll 1$, there is a single rest state (u_0, v_0). A suprathreshold perturbation induces propagation of a wave including abrupt transition from (u_0, v_0) to practically (u_e, v_0) (wave front), slow motion along the right branch of the u-nullcline (wave plateau), abrupt transition to the left branch (wave back), and recovery to the rest state, as illustrated in Fig. 1. In the simplest case such a wave has a planar front and a planar back, which have no common points. If this wave is cut off on both sides, a wave segment is created which contains two phase change points, where the front coincides with the back. The segment will contract laterally and disappear at low excitabil-

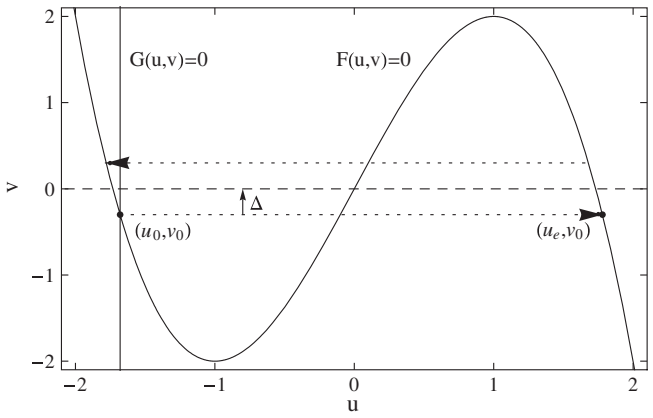

FIG. 1. Phase plane for the excitable system (1) and (2). Solid lines show nullclines, while the dotted line represents the phase trajectory corresponding to a propagating wave. The dashed line corresponds to $v = v^*$.

ity or evolve into two counter rotating spiral waves at high excitability. Consequently, for a given medium excitability there is a wave segment with a particular size and shape, which is intrinsically unstable. In order to make this solution observable it has to be stabilized by an adequate noninvasive feedback control [14]. Note that such stabilized segments represent critical nuclei, from which spiral waves can develop in the medium without the stabilizing feedback. Thus it is of great importance to study the relationship between the shape of these nuclei and the medium excitability. Up to now this study has been restricted to the low excitability limit, where the wave segment size diverges [8,14]. Here a segment transforms into the so-called critical finger, which can be viewed as a spiral wave with infinitely large core. This pattern represents the universal limit of spiral wave propagation derived in [6].

In this Letter, we demonstrate that a free-boundary approach can be used to determine the velocity and the shape of a stabilized wave segment within the whole available excitability range. Moreover, a second universal limit is discovered at the boundary between excitable and bistable media. Here a wave segment transforms into a motionless circular shaped spot. In this limit analytical expressions are derived for the velocity and the size of wave segments. In addition, an interpolation formula for the segment velocity is proposed which is applicable within the whole range between both excitability limits.

The free-boundary approach applied in this study is aimed to simplify the underlying reaction-diffusion model (1) and (2) [6–8]. First, the front and the back of the propagating wave are assumed to be thin in comparison to the wave plateau and, hence, the shape of a wave segment is determined by the boundary of the excited region, e.g., the curve $u(x, y, t) = (u_e + u_0)/2$. It is suitable to specify the shape and the normal velocity of the boundary by the arc length s counted from the phase change point q taking $s > 0$ at the front and $s < 0$ at the back [5].

Second, it is assumed that the normal velocity of the boundary obeys the linear eikonal equation

$$c_n = c_p - Dk, \tag{4}$$

where k is the local curvature and $c_p = c_p(v^{\pm})$ depends on the controller value v^+ (v^-) at the front (back) in accordance with Eq. (3) [5,15,16]. At the phase change point the normal velocity vanishes. However, the velocity of this point in the tangent direction, c_t, is equal to the translational velocity of the whole wave segment as illustrated in Fig. 2. Simple geometry shows that

$$c_p(v^{\pm}) - Dk^{\pm} = c_t \cos(\Theta^{\pm}), \tag{5}$$

where $k^{\pm}$ and $\Theta^{\pm}$ specify the curvature and the normal angle at the front (+) and at the back (−) with respect to the x axis.

Since the wave front is assumed to be thin, the controller value at the whole front is constant $v^+ = v_0$. Hence, the velocity $c_p(v^+)$ in Eq. (5) is also constant $c_p(v^+) = c_p(v_0) \equiv c_0$. In contrast to this, the controller value at the wave back is not constant. Indeed, due to Eqs. (1) and (2) its spatial gradient along the propagation direction is given by $\partial v/\partial x = -\epsilon G(u_e(v), v)/c_t$. Under the assumption $\Delta \ll \Delta_c$, this gradient remains practically constant along the wave plateau, where $G(u_e(v), v) \approx G(u_e(v^*), v^*) \equiv G^*$. Hence, v^- can be written as

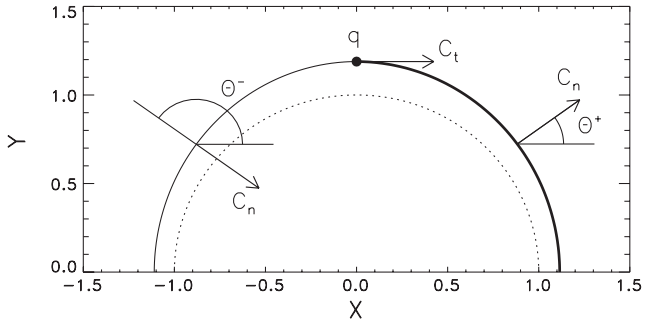

FIG. 2. Shape of a stabilized wave segment computed as the solution of the free-boundary problem (7)–(9) for $C_t = 0.2$ and $B = 0.0367$. The thick (thin) solid line depicts the front (back) above the symmetry axis $Y = 0$. Filled dot indicates the phase change point q. Dotted line represents the circular shaped motionless spot obtained for $B = 0$.

$$v^- = v_0 + \frac{G^*\epsilon}{c_t}[x^+ - x^-]. \tag{6}$$

Here x^+ and x^- determine the locations of the front and the back at the same distance y from the horizontal symmetry axis, where $y = 0$.

It is suitable to use the value c_0 in order to rescale velocities, e.g., $C_t = c_t/c_0$, and space variables, e.g., $S = c_0 s/D$, $X = c_0 x/D$, $Y = c_0 y/D$. Then, since $k^{\pm} = -d\Theta^{\pm}/ds$, Eq. (5) transforms into the dimensionless ordinary differential equation for the angle Θ^+

$$\frac{d\Theta^+}{dS} = -1 + C_t \cos(\Theta^+). \tag{7}$$

Similar transformation taking into account Eq. (6) yields the equation for the angle Θ^-

$$\frac{d\Theta^-}{dS} = \frac{B(X^+ - X^-)}{C_t} - 1 + C_t \cos(\Theta^-), \tag{8}$$

where

$$B = \frac{G^*\epsilon}{\alpha^2\Delta^3}. \tag{9}$$

Equations (7) and (8) supplemented by obvious relationships $dY^{\pm}/dS = -\cos(\Theta^{\pm})$ and $dX^{\pm}/dS = \sin(\Theta^{\pm})$ specify the free-boundary problem for the traveling wave segment. The solution to these equations determines the shape and the velocity of the segment in dependence on the single dimensionless parameter B characterizing the medium excitability.

Note that Eq. (7) can be solved analytically and the Cartesian coordinates of the front can be written as [8]

$$X^+ = \frac{1}{C_t}\ln\frac{1}{1 - C_t\cos(\Theta^+)}, \quad (10)$$

$$Y^+ = -\frac{\Theta^+}{C_t} + \frac{2}{C_t\sqrt{1 - C_t^2}}\arctan\frac{(1 + C_t)\tan\frac{\Theta^+}{2}}{\sqrt{1 - C_t^2}}, \quad (11)$$

that yields, e.g., the segment half-width $W = Y^+(\pi/2)$.

The more complicated Eq. (8) should be integrated numerically in the reverse arc length direction starting at $S = 0$ with $\Theta^- = \pi/2$, $X^- = 0$ and $Y^- = W$, and taking into account that X^+ is determined parametrically by Eqs. (10) and (11). Using a shooting method one must vary the value of B until the corresponding solution satisfies the second boundary condition, $Y^- = 0$, $\Theta^- = \pi$. Repetition of this process for different C_t yields the relationship between B and C_t shown in Fig. 3(a).

In the low excitability limit, where $B \to B_c \approx 0.535$, the velocity C_t obeys the relationship derived in [7,8]

$$C_t = 1 - (B_c - B)/0.63, \quad (12)$$

which is depicted by the dashed line in Fig. 3(a).

In this work we investigate the whole available range $0 \le B \le B_c$. It is found that the linear law (12) fails to describe the dependence $C_t = C_t(B)$ in the limit $B \to 0$, where the transition to a motionless spot is discovered.

In order to analyze this limit, note that in accordance to the eikonal equation (4), a motionless spot should have a circular shape with local curvature $K = 1$. A slowly moving segment, e.g., shown in Fig. 2, has an elliptical-like shape slightly stretched along the Y axis. Based on these data we assume that for $B \ll B_c$ the wave segment exhibits a mirror symmetry with respect to the vertical line crossing the phase change point, i.e.,

$$X^-(-S) = -X^+(S), \quad (13)$$

$$\Theta^+(S) + \Theta^-(-S) = \pi. \quad (14)$$

Moreover, it follows from Eq. (10) that $X^+ = \cos(\Theta^+)$, if $C_t \ll 1$. Substitution of Eqs. (13) and (14) into this expression yields $X^- = \cos(\Theta^-)$. Then Eq. (8) gives

$$\frac{d\Theta^-}{dS} = -1 + (C_t - 2B/C_t)\cos(\Theta^-). \quad (15)$$

Differentiation of Eq. (14) and substitution of both Eqs. (7) and (15) result in the following expression:

$$C_t\cos[\Theta^+(S)] - (C_t - 2B/C_t)\cos[\Theta^-(-S)] = 0. \quad (16)$$

Because of Eq. (14) this equality is valid for any S only if

$$C_t = \sqrt{B}. \quad (17)$$

This square root asymptotics found in the limit $B \to 0$ is shown in Fig. 3(a) by the dotted line. Its substitution into Eq. (11) with $\Theta^+ = \pi/2$ gives the half-width $W(B)$ of the wave segment represented in Fig. 3(b) by the dotted line. Obviously, asymptotics (17) and $W(B)$ based on it are in good quantitative agreement with numerical data for

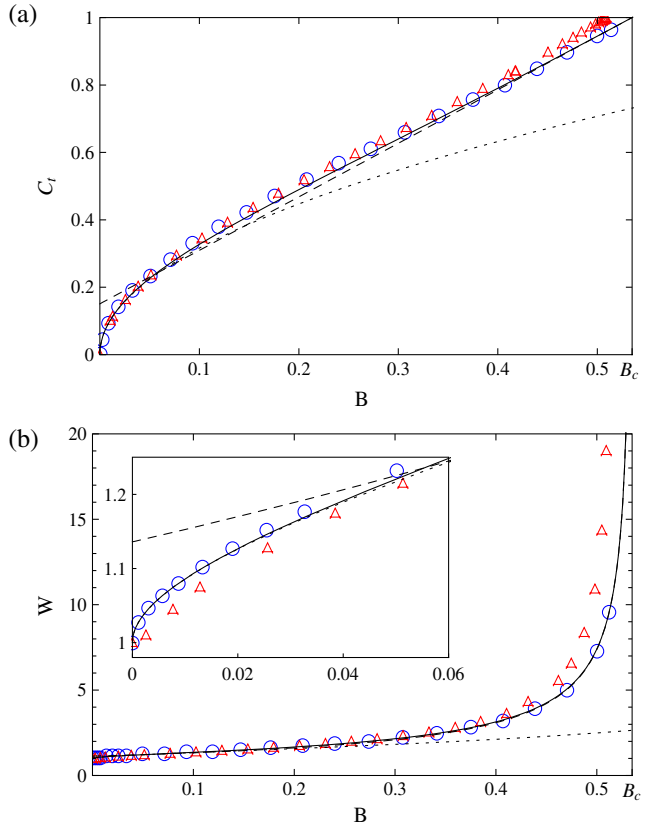

FIG. 3 (color online). Dimensionless velocity C_t and half-width W of a stabilized wave segment vs the parameter B obtained as a solution of the free-boundary problem (7)–(9) (open circles) and from direct integration of the model (1) and (2) (open triangles). (a) Dashed, dotted, and solid lines represent asymptotics (12) and (17) and the interpolation formula (19) for $C_t(B)$, respectively. (b) These functions $C_t(B)$ are substituted into Eq. (11) with $\Theta^+ = \pi/2$ to obtain corresponding relationships $W(B)$ depicted by dashed, dotted, and solid lines.

$B \ll 1$. The analytical expression for the half-width for small B reads

$$W(B) = 1 + \frac{\pi}{4}\sqrt{B} + O(B) \quad (18)$$

and shows that for the motionless segment $W(0) = 1$.

Based on the asymptotics (12) and (17) obtained for the two limiting cases an interpolation formula can be proposed for the whole range $0 \le B \le B_c$ in the form

$$C_t = \sqrt{B + (1 - B_c)\left(\frac{B}{B_c}\right)^n}. \quad (19)$$

If $n = 2.502 \approx 5/2$, it correctly reproduces the asymptotics (17) for $B \to 0$ and the linear law (12) in the vicinity of $B = B_c$ as shown by the solid line in Fig. 3(a). Substitution of Eq. (19) into Eq. (11) with $\Theta^+ = \pi/2$ gives an implicit interpolation formula for the segment half-width W depicted by the solid line in Fig. 3(b).

It is important to compare the results of the free-boundary approach to the numerical integration of the

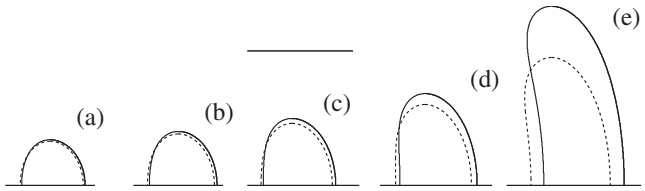

FIG. 4. Boundary of a stabilized wave segment obtained from direct integration of the reaction-diffusion model (1) and (2) (solid lines) and as a solution of the free-boundary problem (7)–(9) (dashed lines). (a) $B = 0.282$, (b) $B = 0.334$, (c) $B = 0.385$, (d) $B = 0.436$, (e) $B = 0.488$. Horizontal bar length 5.

underlying reaction-diffusion equations (1) and (2) with fixed $\delta = -1.6797$, $D = 1$, and $0 < \epsilon < 0.002$. The integration is performed with explicit Euler scheme with $\Delta x = 0.1$ and $\Delta t = 0.001$. The computations are carried out within a frame containing 500×1200 nodes comoving with a wave segment. To realize a stabilizing feedback the control signal $I(t)$ is taken to be proportional to the coordinate y_q of the phase change point

$$I(t) = k_{fb}[y_q(t) - W_d], \tag{20}$$

where W_d is the desired half-width of the wave segment and k_{fb} is the feedback strength. In the vicinity of B_c this signal obtained for $k_{fb} = 5 \times 10^{-5}$ is used to change the parameter ϵ in accordance to $\epsilon = \bar{\epsilon} + I(t)$ [14]. However, for $B \ll B_c$ it is more efficient to affect the diffusion constant D taking $D = 1 + I(t)$ and using $k_{fb} = 0.5$.

The velocity and the half-width of stabilized segments resulting from the numerical integrations of the Eqs. (1) and (2) are also shown in Fig. 3 in comparison to the data obtained in the framework of the free-boundary approach. In Fig. 4 the boundaries of the stabilized wave segments are compared to the solutions of the free-boundary problem. It can be seen that the segment velocity is predicted with 5% accuracy within the whole excitability range. The accuracy of the half-width predictions is better than 8% for $B < 0.4$. However, for $B \approx B_c$ the segment half-width computed from the model (1) and (2) becomes remarkably larger than the predicted one, since it diverges at $B \approx 0.517 < B_c = 0.535$. Higher-order correction terms are responsible for this small deviation from the theoretically predicted value B_c [6].

In summary, the translational motion of a stabilized wave segment in an excitable medium described by the generic reaction-diffusion model (1) with $D_v = 0$ is analyzed in the framework of a free-boundary approach. It is shown that for $\Delta \ll \Delta_c$ (sufficient condition) the free-boundary problem can be reduced to the system of ordinary differential equations (7) and (8) containing a single dimensionless parameter B characterizing the medium excitability. In the low excitability limit, $B \to B_c$, which has been analyzed earlier [6–8], the half-width W of the wave segment diverges and it transforms into a critical finger. Here the second universal limit, $B \to 0$, is discovered, which corresponds to the transformation of a moving segment into a circular shaped motionless spot, that represents the critical nucleus in bistable media. It is analytically proven that for $B \ll B_c$ the segment velocity C_t and the half-width W obey the asymptotics (17) and (18), respectively. The formula (19) describes the segment velocity within the whole range between two excitability limits. Since this formula does not depend on details of the local kinetics, it can be applied to analyze the velocity and the shape of wave segments in a variety of excitable media. Moreover, parameter B can be expressed through experimentally measurable characteristics of an excitable medium such as the velocity and the duration of a propagating pulse [17].

Note that traveling spots intensively studied in the system (1) with $D_v \gg D$ [10,11] differ very strongly from wave segments described above for the case $D_v = 0$. However, the motionless spot corresponding to $\epsilon = 0$ is obviously the same in both cases. Thus, there are nontrivial transitions in segment dynamics under variations of ϵ and D_v that are a challenge for future studies.

We thank the Deutsche Forschungsgemeinschaft (SFB 555) for supporting this research.

[1] A. T. Winfree, *The Geometry of Biological Time* (Springer, Berlin Heidelberg, 2000).
[2] A. S. Mikhailov, *Foundations of Synergetics* (Springer, Berlin Heidelberg, 1994).
[3] *Chemical Waves and Patterns*, edited by R. Kapral and K. Showalter (Kluwer, Dordrecht, 1995).
[4] H. Engel, F.-J. Niedernostheide, H.-G. Purwins, and E. Schöll, *Self-Organization in Activator-Inhibitor Systems: Semiconductors, Gas Discharge, and Chemical Active Media* (Wissenschaft & Technik, Berlin, 1996).
[5] V. S. Zykov, *Simulation of Wave Processes in Excitable Media* (Manchester Univ. Press, Manchester, 1987).
[6] A. Karma, Phys. Rev. Lett. **66**, 2274 (1991).
[7] V. Hakim and A. Karma, Phys. Rev. E **60**, 5073 (1999).
[8] V. S. Zykov and K. Showalter, Phys. Rev. Lett. **94**, 068302 (2005).
[9] A. Turing, Phil. Trans. R. Soc. B **237**, 37 (1952).
[10] T. Ohta, M. Mimura, and R. Kobayashi, Physica (Amsterdam) **34D**, 115 (1989).
[11] K. Krischer and A. Mikhailov, Phys. Rev. Lett. **73**, 3165 (1994).
[12] E. Mihaliuk, T. Sakurai, F. Chirila, and K. Showalter, Faraday Discuss. **120**, 383 (2002).
[13] T. Sakurai, E. Mihaliuk, F. Chirila, and K. Showalter, Science **296**, 2009 (2002).
[14] V. S. Zykov, Eur. Phys. J. Special Topics **157**, 209 (2008).
[15] J. J. Tyson and J. P. Keener, Physica (Amsterdam) **32D**, 327 (1988).
[16] A. M. Pertsov, M. Wellner, and J. Jalife, Phys. Rev. Lett. **78**, 2656 (1997).
[17] V. S. Zykov, Physica (Amsterdam) **238D**, 931 (2009).